

Route of hydrodynamic turbulence in rotating shear flow: Secondary perturbation triggers growing eigenmodes through the elliptical instability

Banibrata Mukhopadhyay

*Institute for Theory and Computation, Harvard-Smithsonian Center for Astrophysics,
60 Garden Street, MS-51, Cambridge, MA 02138*

Origin of hydrodynamic turbulence in rotating shear flow, e.g. plane Couette flow including the Coriolis force, is a big puzzle. While the flow often exhibits turbulence in laboratory experiments, according to the linear perturbation theory it should always be stable. We demonstrate that the secondary disturbance to the primarily perturbed flow triggers the elliptical instability in such a system and hence an exponential growing eigenmode. This result has an immediate application to astrophysics and geophysics which often exhibit a turbulent flow with the Keplerian angular momentum profile. We address the origin of turbulence in such a Keplerian flow which is similar to rotating Couette flow.

PACS numbers: 47.20.-k, 47.20.Lz, 47.20.Ft, 92.10.Lq

Despite of many efforts devoted, the origin of hydrodynamic turbulence is still poorly understood. One of the main problems behind this is that there is a significant mismatch between the predictions of linear theory and experimental data. For example, in the case of plane Couette flow, laboratory experiments and numerical simulations show that the flow may be turbulent for a Reynolds number, $R \sim 350$, while according to the linear theory the flow should be stable for all R . Similar mismatch between theoretical results and observations is found in geophysical and astrophysical contexts, where the accretion flow of neutral gas with Keplerian angular momentum profile is a common subject. A Keplerian accretion disk flow having a very low molecular viscosity must generate turbulence and successively diffusive viscosity, which support transfer of mass inward and angular momentum outward. However, theoretically this flow never exhibits any unstable mode which could trigger turbulence in the system. On the other hand, laboratory experiments of Taylor-Couette systems, which are similar to Keplerian disks, seem to indicate that although the Coriolis force delays the onset of turbulence, the flow is ultimately unstable to turbulence for Reynolds numbers larger than a few thousand [1], even for subcritical systems. Longaretti [2] reviews the experimental evidence for the existence of turbulence in subcritical laboratory systems, and concludes, based on phenomenological analogy, that a similar process must happen in astrophysical accretion flows. Indeed, Bech & Anderson [3] see turbulence persisting in numerical simulations of subcritical rotating flows for large enough Reynolds numbers.

How does shearing flow that is linearly stable to perturbations switch to a turbulent state? Since last decade, many authors have come forward with a possible explanation of this fact, based on *bypass* transition (see [4, 5, 6, 7, 8, 9] and references therein), where the decaying linear modes show an arbitrarily large transient energy growth at a suitably tuned perturbation. In lieu of linear instabilities e.g. magnetorotational instability,

the transient energy growth, supplemented by a non-linear feedback process to repopulate the growing disturbance, could plausibly sustain turbulence for large enough Reynolds numbers.

However, in the case of rotating shear flow, e.g. Couette-Taylor flow, Keplerian accretion flow, the transient energy growth is insignificant for three-dimensional perturbations. The Coriolis effect, which absorbs the pressure fluctuation, is the main culprit to kill any growth of energy. Nevertheless, at a very large Reynolds number, certain two-dimensional perturbations may produce large transient growth in such a flow. However, in two-dimension, the underlying perturbations must ultimately decline to zero in the presence of viscosity [8, 9]. To overcome this limitation, it is necessary to invoke three-dimensional effects. Various kinds of secondary instabilities, such as the elliptical instability, are widely discussed as a possible route to self-sustained turbulence in linearly perturbed shear flows (see, e.g. [10, 11, 12, 13, 14, 15, 16, 17, 18]). These effects, which generate three-dimensional instabilities of a two-dimensional flow with elliptical streamlines, have been proposed as a generic mechanism for the breakdown of many two-dimensional high Reynolds number flows whose vortex structures can be locally seen as elliptical streamlines. However, to our knowledge, such effects have not been discussed properly in literatures for rotating Keplerian flows which have a vast application to various natural phenomena. More than a decade ago, the possible role of the elliptical instability in astrophysical accretion disk physics was first explored [19] and it was shown that angular momentum may be transferred from the disk to the tidal source by the instability effect [20, 21]. Therefore, naturally we are motivated to see whether these three-dimensional instabilities are present in rotating shear flows which consist of elliptical streamlines under two-dimensional perturbation. We plan to show that in presence of secondary effects, three-dimensional perturbation can generate large growth and

presumably trigger turbulence in rotating shear flows. Unlike the growth of transient kind which is significant in two-dimension only, in the present case it is essentially the three-dimensional effects which produce large growth. Possibility of large growth in shear flows with *rotation* by three-dimensional perturbation opens a new window to explain hydrodynamic turbulence.

Let us consider a small patch of rotating shear flow whose unperturbed velocity profile corresponds to a linear shear of the form $\vec{U}_0 = (0, -x, 0)$. Because of rotation, a Coriolis acceleration acts on the fluid element having angular frequency $\vec{\Omega} = (0, 0, \Omega_3)$ where according to choice of our units $\Omega_3 = 1/q$. The parameter q is positive, describing the radial dependence of $\Omega(r) = \Omega_0(r_0/r)^q$ (see [9] for detail). We choose all the variables to be dimensionless. When the Reynolds number is very large, this flow exhibits a large transient growth under a suitable two-dimensional perturbation [9] which modifies the linear shear profile as

$$\begin{aligned}\vec{U} &= \vec{U}_0 + \vec{w} = (w_x, -x + w_y, 0) = \mathbf{A} \cdot \vec{d}, \\ w_x &= \zeta \frac{k_y}{\kappa^2} \sin(k_x x + k_y y), \quad w_y = -\zeta \frac{k_x}{\kappa^2} \sin(k_x x + k_y y),\end{aligned}\quad (1)$$

where \vec{d} is the position vector and \mathbf{A} is a tensor of rank 2. Now expanding the $\sin(k_x x + k_y y)$ terms and choosing a small patch, \mathbf{A} is given by

$$\mathbf{A} = A_j^k = \begin{pmatrix} \zeta \sqrt{\epsilon(1-\epsilon)} & \zeta(1-\epsilon) & 0 \\ -(1+\zeta\epsilon) & -\zeta \sqrt{\epsilon(1-\epsilon)} & 0 \\ 0 & 0 & 0 \end{pmatrix}, \quad (2)$$

where $\epsilon = (k_x/\kappa)^2$, $\kappa = \sqrt{k_x^2 + k_y^2}$, and ζ is the amplitude of vorticity perturbation. Here $k_x = k_{x0} + k_y t$, which basically is the radial component of wave-vector, varies from $-\infty$ to $+\infty$, where k_{x0} is a large negative number. The above plane wave typed perturbation is frozen into the fluid and is sheared along with the background flow. At $t = 0$, the effective wave vector of perturbation in the x direction (k_x) is negative, which provides very asymmetric leading waves. As time goes on, the wavefronts are straightened out by the shear and $|k_x|$ decreases. At the time when the transient growth is maximum, $k_x \sim 0$ and the wavefronts become almost radial. At yet later time, the growth decreases and the wave becomes of a trailing pattern. Clearly \vec{U} describes a flow having generalized elliptical streamlines with ϵ , a parameter related to the measure of eccentricity [22], runs from 0 to 1 as the perturbation evolves. Now we plan to study how does this perturbed shear flow behave under the further perturbation, namely a *secondary perturbation*.

The linearized equations for the evolution of a secondary perturbation \vec{u} , such that $\vec{U} \rightarrow \vec{U} + \vec{u}$, to the flow are

$$\begin{aligned}(\partial_t + \vec{U} \cdot \nabla) \vec{u} + \vec{u} \cdot \nabla \vec{U} + 2\vec{\Omega} \times \vec{u} &= -\nabla \tilde{p} + \frac{1}{R} \nabla^2 \vec{u}, \\ \nabla \cdot \vec{u} &= 0\end{aligned}\quad (3)$$

where \tilde{p} is pressure in the fluid element and R is the Reynolds number. A secondary perturbation of the plane wave kind is given by

$$(u_i, \tilde{p}) = (v_i(t), p(t)) \exp(ik_m(t)x^m), \quad (4)$$

where the Latin indices, run from 1 to 3, indicate the spatial components of a variable, e.g. $x^m \equiv (x, y, z)$. Therefore, after some algebra, we obtain the evolution of a linearized secondary perturbation

$$\dot{v}_j + A_j^k v_k + 2\epsilon_{mkj} \Omega^m v^k = -ip k_j - \frac{v_j}{R} k^2, \quad (5)$$

$$\dot{k}_j = -(A_j^m)^T k_m, \quad k^n \dot{v}_n = k^m A_m^n v_n, \quad (6)$$

where ‘over-dot’ indicates a derivative with respect to t , ϵ_{mkj} is a Levi-Civita tensor, and $k^2 = k_m k^m$. A similar set of equations was obtained by Bayly [11], except that they now have additional terms induced due to the Coriolis and the viscous effects along with a modified \mathbf{A} . For a fixed k_x , the components k_1 and k_2 of wave-vector [$\vec{k} = k_m = (k_1, k_2, k_3)$] of secondary perturbation oscillate in time with the angular frequency $\varpi = \sqrt{\zeta(1-\epsilon)}$, while the vertical component, k_3 , is constant. As we choose the signature of the background Minkowski space-time to be $[-, +, +, +]$, it does not matter whether any Latin index appears as a lower case or an upper case. For example, $A_j^k = A_{jk}$, where j and k indicate the row number and the column number of the associated matrix respectively. Projecting out eqn. (5) by $P_i^j = \delta_i^j - k^{-2} k^j k_i$ and using eqn. (6), we obtain

$$\begin{aligned}\dot{v}_i &= \left(2 \frac{k^j k_i}{k^2} - \delta_i^j\right) A_j^k v_k - 2\epsilon_{mki} \Omega^m v^k - \frac{v_i}{R} k^2 \\ &\quad + \left(2\epsilon_{mkj} \Omega^m v^k + \frac{v_j}{R} k^2\right) \frac{k^j k_i}{k^2}.\end{aligned}\quad (7)$$

Now we specifically concentrate on the flow having low viscosity. Therefore, we neglect the viscous term in eqn. (7) comparing others and rewrite

$$\dot{v}_i = \Lambda_{ij}^j v_j, \quad \Lambda_{ji} = \begin{pmatrix} \left(\frac{2k_1^2}{k^2} - 1\right) A_{11} + \frac{2k_1 k_2}{k^2} (A_{21} + \Omega_3) & \frac{2k_1^2}{k^2} (A_{12} - \Omega_3) + 2\Omega_3 - A_{12} + \frac{2k_1 k_2}{k^2} A_{22} & 0 \\ \frac{2k_1 k_2}{k^2} A_{11} + \frac{2k_2^2}{k^2} (A_{21} + \Omega_3) - A_{21} - 2\Omega_3 & \frac{2k_1 k_2}{k^2} (A_{12} - \Omega_3) + \left(\frac{2k_2^2}{k^2} - 1\right) A_{22} & 0 \\ \frac{2k_1 k_3}{k^2} A_{11} + \frac{2k_2 k_3}{k^2} (A_{21} + \Omega_3) & \frac{2k_1 k_3}{k^2} (A_{12} - \Omega_3) + \frac{2k_2 k_3}{k^2} A_{22} & 0 \end{pmatrix}. \quad (8)$$

The general solution of eqn. (8) for a particular k_x can be written as a linear superposition of Floquet modes

$$v_i(t) = \exp(\sigma t) f_i(\phi), \quad (9)$$

where $\phi = \varpi t$, $f_i(\phi)$ is a periodic function having time-period $T = 2\pi/\varpi$, and σ is the Floquet exponent which is the eigenvalue of the problem. As k_x varies, ϵ changes, therefore the eigenvalue changes. Clearly, if σ is positive then the system is unstable. To compute σ , one has to evaluate the elements of a matrix $M_{mi}(2\pi)$ whose eigenvalues and eigenvectors are respectively $e^{\sigma T}$ and $f_i(2\pi)$, while $M_{mi}(\phi)$ itself satisfies

$$\frac{dM_{ji}(t)}{dt} = \Lambda_j^m M_{mi}(t), \quad (10)$$

with the condition $M_{ji}(0) = \delta_{ji}$. Clearly, (10) is the evolution equation of velocity. If μ is a real positive eigenvalue of $M_{mi}(2\pi)$, then the corresponding $\sigma = \ln(\mu)/T$. One can evaluate μ by an elementary numerical technique. However, eqn. (10) has exact analytical solution for an initial perturbation $\vec{k}_0 = (0, 0, 1)$. In this case, \vec{k} remains constant throughout for a fixed ϵ and therefore the growth rate, σ , is the highest eigenvalue of Λ_j^m given by

$$\sigma = \sqrt{\zeta\epsilon - (2\Omega_3 - 1)(2\Omega_3 - \zeta)}. \quad (11)$$

- When $\Omega_3 = 0$, $\sigma = \sqrt{\zeta(\epsilon - 1)}$. This verifies that non-rotating two-dimensional shear flow is always hydrodynamically stable under a *pure* vertical perturbation.

- When $\Omega_3 = 1/2$, $\sigma = \sqrt{\zeta\epsilon}$. Therefore, rotating shear flow with a constant angular momentum profile is always hydrodynamically unstable. The energy growth rate of perturbation increases with the strain rate, i.e. eccentricity, of the flow.

- When $\Omega_3 = 2/3$, $\sigma = \sqrt{\zeta\epsilon - (4 - 3\zeta)/9}$. Therefore, a Keplerian flow with elliptical streamlines is hydrodynamically unstable under a *pure* vertical perturbation, only if $\zeta > 1/3$.

However, apart from the vertical one, there are some other three-dimensional perturbations [23] which can generate instability in rotating shear flows with $\zeta < 1/3$, that we describe by numerical solutions. We essentially focus on the Keplerian flow when $q = 3/2$. As primary perturbation evolves with time, eccentricity decreases, and then energy growth rate due to secondary perturbation changes. Figure 1a shows the variation of maximum growth rate, σ_{max} , as a function of eccentricity parameter, ϵ , for various values of ζ , the amplitude of

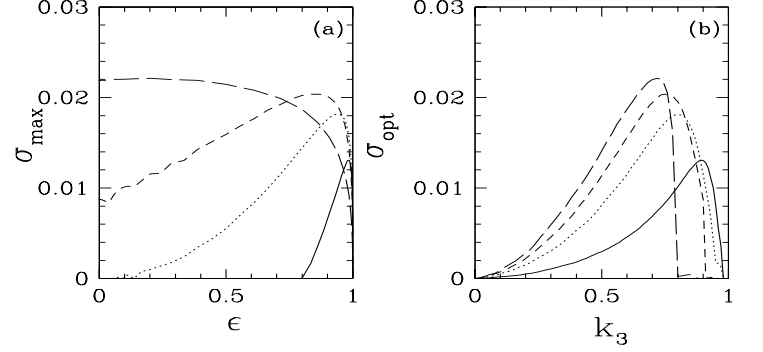


FIG. 1: (a) Variation of maximum growth rate as a function of eccentricity parameter when solid, dotted, dashed and long-dashed curves indicate the results for $\zeta = 0.2, 0.1, 0.05, 0.01$ respectively. (b) Variation of optimum growth rate as a function of vertical component of perturbation wave-vector when various curves are same as of (a). $q = 3/2$ throughout.

primary perturbation, in the Keplerian flows. By “maximum” we refer the quantity obtained by maximizing over the vertical component of wave-vector, k_3 . While a vertical perturbation gives rise to the best growth rate for $\zeta > 1/3$, as we show above analytically, for $\zeta < 1/3$ other three-dimensional perturbations maximize growth rate. At small ϵ and large ζ , the streamlines of the flow essentially become circular (see eqn. (2)), and thus in absence of any significant elliptical effect growth rate severely decreases. On the other hand, when ϵ and ζ both are small, the background reduces to plane shear structure and therefore any growth arises due to primary perturbation only.

Figure 1b shows the variation of optimum growth rate, σ_{opt} , as a function of k_3 for various values of ζ , in the Keplerian flows. By “optimum” we refer the quantity obtained by maximizing over ϵ . Interesting fact to note is that the optimum growth rate is obtained always for three-dimensional perturbation with significant vertical effect, i.e. a non-zero value of k_3 . Moreover, as ζ increases, instability occurs at larger ϵ with higher k_3 . Therefore, three-dimensional elliptical instability is more prompt at larger ζ .

Above results verify that at a range of ϵ the *instantaneous* three-dimensional growth rate due to secondary perturbation is always real and positive, which motivates us to compute the actual growth itself during simultaneous evolution of both the perturbations. As primary perturbation evolves, k_x varies with time and therefore

A does so. Thus, in reality, the wave-vector of secondary disturbance is no longer periodic, though the corresponding equation (6) is still valid. To compute growth in energy one has to find out the elements of a matrix

$$\mathcal{M}_{ik}(t) = M_{im}(t)^T M_{mk}(t) \quad (12)$$

whose largest eigenvalue is growth in energy at a time t . Clearly, $\mathcal{M}_{ik}(t)$ is the instantaneous energy of the flow. k_x and k_1 start with a large negative value when the flow is highly eccentric. With time k_x (as well as k_1) decreases in magnitude and finally becomes zero when the streamlines become circular. If $\zeta = 0$, then k_x is same as k_1 . However, for $\zeta > 0$, k_1 increases faster than k_x , as follows from eqn. (6), and becomes positive during the evolution of perturbation. When $k_1 \rightarrow 0$, growth maximizes.

Figure 2a shows the variation of growth as a function of t for various values of ζ . Note that as ζ increases, growth maximizes at an earlier time. Figure 2b shows the variation of maximum growth as a function k_3/k_2 . The quantity k_3/k_2 carries information about how three-dimensional the flow is. We know that in two-dimensional plane shear flow the maximum growth, G_{max} , scales with k_{x0}^2 [9]. However, for $\zeta > 0$, G_{max} decreases at small k_3/k_2 , while increases at large k_3/k_2 . This clearly proves that three-dimensional secondary perturbation triggers elliptical instability which produces larger growth. As k_{x0} and k_{10} ($\sim R^{1/3}$ [8, 9]) increase, the effects due to elliptical instability increase, and thus the corresponding growth does so. When $k_{x0} = k_{10} = -10^3$, $G_{max} \sim 4 \times 10^4$ at $k_3/k_2 = 1$ for $\zeta = 0.1$, which is an order of magnitude larger compared to that for $\zeta = 0$. If we consider a smaller R with the corresponding $k_{x0} = k_{10} = -10^2$, then G_{max} at $k_3/k_2 = 1$ decreases to $\sim 2 \times 10^3$ for $\zeta = 0.1$, which is still a factor of two larger compared to that for $\zeta = 0$. Therefore, this is confirmed without any doubt that three-dimensional elliptical instability efficiently triggers turbulence in shear flows.

When t increases from 0 to $t_{max} = -k_{x0}/k_y$, $k_x(t)$ varies from k_{x0} ($\sim -\infty$) to 0, and ϵ decreases from 1 to 0. Note that $G_{max} \sim 2 \times 10^3 - 4 \times 10^4$ when $k_{10}^3 \sim R \sim 10^6 - 10^9$. As this large growth is the result of three-dimensional perturbation, even in presence of viscosity the underlying perturbation effect should survive. Presumably, this growth factor is enough to trigger non-linear effects and turbulence in such flows. There are many important natural phenomena where the Reynolds number is very large. In astrophysical accretion disks R always could be $10^{10} - 10^{14}$ [9] because of their very low molecular viscosity. Therefore, the present mechanism can have a very good application to such disk flows to explain their *turbulence puzzle* when it is cold and neutral in charge. On the other hand, we argue that the subcritical transition to turbulence in Couette flow may be the result of secondary perturbation which triggers

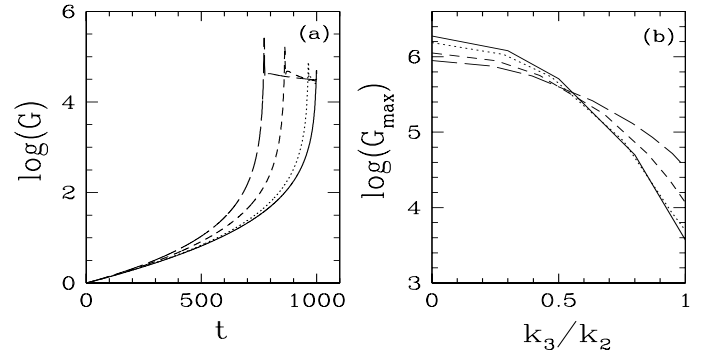


FIG. 2: (a) Variation of growth as a function of time due to simultaneous evolution of both perturbations, when $k_3 = 0.8$. Solid, dotted, dashed and long-dashed curves indicate the results for $\zeta = 0, 0.01, 0.05, 0.1$ respectively. (b) Variation of maximum growth as a function of k_3/k_2 , when various curves are same as of (a). Other parameters are $k_{x0} = k_{10} = -1000$, $k_{20} = 1$, and $q = 3/2$.

elliptical instability modes in the system. It is to be seen now whether all shear flows, exhibit subcritical turbulence in the laboratory, do also exhibit large growth due to secondary perturbation, according to the present mechanism.

The author is grateful to Ramesh Narayan for suggesting this problem and for extensive discussion and encouragement throughout the course of the work. This work was supported in part by NASA grant NNG04GL38G and NSF grant AST 0307433.

-
- [1] D. Richard, & J.-P. Zahn, *A&A* **347**, 734 (1999).
 - [2] P. Longaretti, *ApJ* **576**, 587 (2002).
 - [3] K. Bech, & H. Andersson, *J. Fluid Mech.* **347**, 289 (1997).
 - [4] K. Butler, & B. Farrell, *Phys. Fluids A* **4**(8), 1637 (1992).
 - [5] S. Reddy, & D. Henningson, *J. Fluids Mech.* **252**, 209 (1993).
 - [6] L. Trefethen, A. Trefethen, S. Reddy, & T. Driscoll, *Science* **261**, 578 (1993).
 - [7] G. Chagelishvili, J.-P. Zahn, A. Tevzadze, & J. Lominadze, *A&A* **402**, 401 (2003).
 - [8] O. Umurhan, & O. Regev, *A&A* **427**, 855 (2004).
 - [9] B. Mukhopadhyay, N. Afshordi, & R. Narayan, *ApJ* **629**, 383 (2005); N. Afshordi, B. Mukhopadhyay, & R. Narayan, *ApJ* **629**, 373 (2005).
 - [10] R. Pierrehumbert, *Phys. Rev. Lett.* **57**, 2157 (1986).
 - [11] B. Bayly, *Phys. Rev. Lett.* **57**, 2160 (1986).
 - [12] A. Craik, & W. Criminalle, *Proc. R. Soc. London Ser. A* **406**, 13 (1986).
 - [13] M. Landman, & P. Saffman, *Phys. Fluids* **30**(8), 2339 (1987).
 - [14] C. Hellberg, & S. Orszag, *Phys. Fluids* **31**(1), 6 (1988).
 - [15] F. Waleffe, *Phys. Fluids A* **2**(1), 76 (1989).
 - [16] A. Craik, *J. Fluid Mech.* **198**, 275 (1989).

- [17] S. Le Diześ, M. Rossi, & K. Moffatt, *Phys. Fluids* **8(8)**, 2084 (1996).
- [18] R. Kerswell, *Ann. Rev. Fluid Mech.* **34**, 83 (2002).
- [19] J. Goodman, *ApJ* **406**, 596 (1993).
- [20] S. Lubow, J. Pringle, & R. Kerswell, *ApJ* **419**, 758 (1993).
- [21] D. Ryu, & J. Goodman, *ApJ* **422**, 269 (1994).
- [22] Note that ϵ is a parameter related to the measure of eccentricity but not the eccentricity itself.
- [23] By vertical perturbation we mean that only the vertical component of initial perturbation wave-vector is non-zero, while any perturbation with a non-zero vertical component of initial wave-vector is called three-dimensional perturbation.